Available online at www.sciencedirect.com

SCIENCE DIRECT®

Journal of Nuclear Materials 341 (2005) 224–230

journal of nuclear materials

www.elsevier.com/locate/jnucmat

NIR Raman spectrometer for monitoring protonation reactions in gaseous hydrogen

Jacek Borysow [a,*], Manfred Fink [b]

[a] *Department of Physics, Michigan Tech. University, Houghton, Michigan 49931, USA*
[b] *Department of Physics, The University of Texas at Austin, Austin, Texas 78712, USA*

Received 9 March 2004; accepted 22 February 2005

Abstract

Spontaneous Raman spectroscopy was used to monitor molecular hydrogen isotope exchange reactions between H_2, D_2, and HD. A tunable 780 nm, multimode laser diode with power output between 300 and 500 mW served as the excitation source. Hydrogen isotopes could be detected at partial pressure of 13 Pa (number density 3.2×10^{21} m^{-3}) at total gas pressure of 5.3×10^{4} Pa (number density 1.3×10^{25} m^{-3}) with signal-to-noise better than 2 during minutes long observations. The high sensitivity was achieved using multiple pass cell in conjunction with atomic vapor Rb absorption filter employed to eliminate Rayleigh scattered laser light. We have used the new spectrometer to measure the rapid isotope exchange reactions taking place in the palladium hydrogen purifier.

1. Introduction

One of the major elements in tritium processing systems is hydrogen isotopes identification and separation. Work with multiple hydrogen isotopes at the same time is often accompanied by isotopic mixing. Formation of HD and TH, molecules as a result of interaction between the material surface in gaseous hydrogen isotopes mixtures of H_2, D_2 and T_2 have been the subject of many studies [1–4]. The partial pressures of the species are usually monitored with a mass spectrometer. However, mass spectrometry and gas chromatography differentiate poorly between HT and D_2. Laser Raman spectrometry offers excellent differentiation among hydrogen isotopomers containing tritium and deuterium but offers only modest sensitivity. Taylor et al. [5] reported recently the use of Raman spectroscopy for real-time analysis of tritiated gases. The authors demonstrated a detection limit for hydrogen in ambient-pressure gas mixtures of about ten parts-per-million with unity signal-to-noise ratio in a one minute analysis period. They achieved high sensitivity using an actively stabilized external resonator, whose length was matched to the single-frequency excitation of 5 W Nd:YVO_4 laser operating at 532 nm.

In this paper we describe Raman system which offers about factor of 10 lower detection limits than ones reported by Taylor et al. [5]. Its greatest advantage is low cost and simplicity.

We demonstrated its performance by measuring traces of HD in H_2 and D_2 and production of HD in H_2, D_2, and HD mixtures in the presence of palladium membrane hydrogen purifier.

---

[*] Corresponding author. Tel.: +1 906 370 5715.
E-mail address: jborysow@mtu.edu (J. Borysow).

0022-3115/$ - see front matter © 2005 Elsevier B.V. All rights reserved.
doi:10.1016/j.jnucmat.2005.02.002

2. Experiment

All our experiments were performed using a setup similar to one first described by Fink [6] and presented in Fig. 1(a) and (b). The optics is shown in Fig. 1(a) and the gas handling/vacuum system is depicted in Fig. 1(b). The isotope exchange experiments were carried out with the use of Gas Technologies model HP-4 hydrogen purifier. Experiments aimed at determining the detection limits of hydrogen isotopes by direct gas

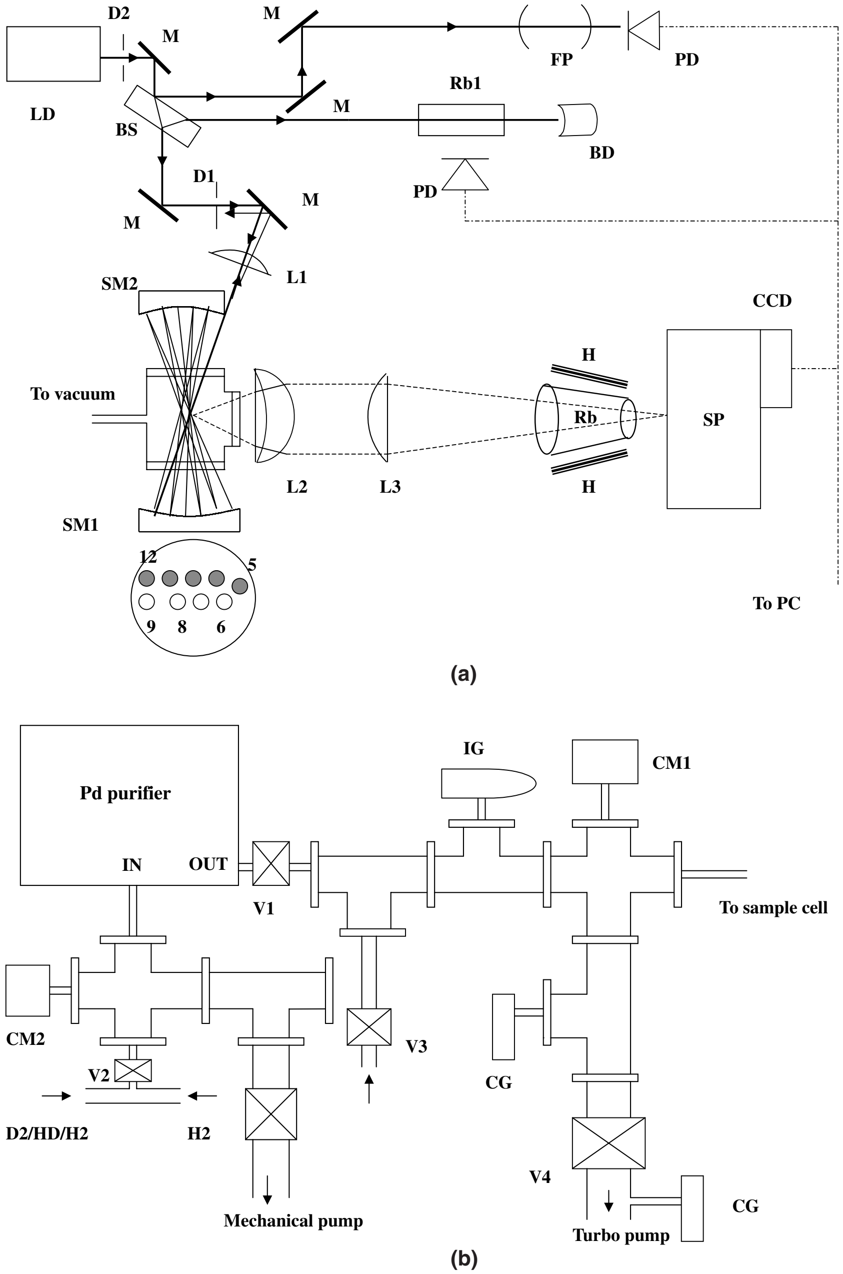

Fig. 1. (a) Experimental setup: optics. LD – tunable laser diode, M – dielectric mirrors, FP – scanning Fabry–Perot confocal interferometer, Rb – cell with rubidium, Rb1 – heated cell with rubidium, PD – photodiode, BS – glass beam splitter, D1, D2 – diaphragms, SM1, SM2 – high reflective, concave spherical mirrors of radius of 100 mm, and diameter 50.2 mm, Rb – cell with rubidium in Ar as a buffer gas, H – heaters, L1, L2, L3 – lenses, SP – spectrograph, CCD – CCD camera, BD – beam dump. (b) Experimental setup: Gas handling system. V1, V2, V3, V4 – manual valves, CM1 – 1330 Pa head, capacitance manometer, CM2 – 10^5 Pa head, capacitance manometer, CG – convectron pressure gauge, IG – Ion pressure gauge.

mixing of trace amounts HD and D_2 with H_2 that bypassed the hydrogen purifier. Valve *V*1 in Fig. 1(b) was closed during all sensitivity measurements. The gases were transported in a vacuum system built from standard stainless steel with 38.1-mm internal diameter conflat components and copper gaskets between flanges. The sample cell was connected to the vacuum system via a #7 *ACE Glass Co.* threaded quick connector. The system was pumped down to 10^{-6} Pa by 80 l/s turbo molecular pump before experiments. The major components of Raman apparatus are:

(1) Laser diode (LD) tuned to the D2 line of rubidium near 780 nm.
(2) Pair of 50.2-mm diameter concave mirrors (*SM*1, *SM*2) made out of BK7 glass with 100.0-mm radius of curvature, separated by a distance of about 200 mm. The nominal reflectivity of the mirrors at normal incidence is better that 99.99%.
(3) Sample cell made out of 1.4-mm thick Pyrex glass with 36.0-mm diameter front window. The outer diameter of the cell is 36.0 mm and its length is 56.0 mm. The side windows are made of fused silica and are coated with antireflection coating centered at 790 nm with nominal reflectivity at normal angle of incidence smaller than 0.01% per surface. The windows are glued to the sample cell by means of vacuum epoxy.
(4) Collection optics ($L1, L2$).
(5) A 0.275-m spectrograph (SP) coupled to a cooled CCD camera. The heated rubidium (Rb) cell in front of the entrance slit of spectrograph filters out most of the Rayleigh scattered light. We use Rb cell developed by Sabbaghzadeh [7]. Typical suppression of the Rayleigh line is about 1000.

The gas used in all measurements was a combination of pure hydrogen and addition of a mixture of H_2, D_2, and HD, from a bottle of unknown origin. Hydrogen gas was research purity rated at 99.998% The composition of the additive mixture was analyzed in house by means of mass spectrometry and yielded H_2:D_2:HD ratio 2.8:100:19.9.

2.1. Laser system

We used a commercial tunable laser system (SDL 8630). The gain element chip in this laser was a tapered amplifier glued to a matched-length heat sink. It provides access to both antireflective coated facets. The tuning element was an optical grating in Littrow configuration. Once tuned to the rubidium D_2 line frequency the laser drift was smaller that 1.0 GHz per hour with no active locking frequency mechanism. The fluorescence monitored by the photodiode from the rubidium reference cell *Rb*1 was used to tune the laser to Rb D_2 line. The laser was equipped with beam shaping optics. The beam intensity profiles of focused spot closely resembled Gaussian profiles in both horizontal and vertical directions. In general, it was possible to adjust operating current, grating position and laser chip temperature to operate the laser in single longitudinal mode. However, during most experiments we could see up to three modes separated by approximately 2 GHz corresponding to the length of the external laser cavity. The mode structure was monitored by scanning confocal Fabry–Perot interferometer with 7.5 GHz free spectral range and finesse of 200 denoted as *FP* in Fig. 1(a). Typically laser power was set to 350 mW out of maximum 500 mW available from the laser. The laser was polarized parallel to the table plane.

2.2. Multi-pass configuration

The multi-pass cell used in all our experiments was first described by Kiefer [8] and later extensively used by Fink [7,9]. In our configuration the laser beam is focused by 120-mm focal length plano convex lens *L*1 at the distance equal to two focal lengths from the spherical concave mirror *SM*1. The focus is subsequently imaged at the same place after reflection from mirror *SM*2. On typical day we had 40 passes through the focal area between the two mirrors. After last reflection, laser beam leaves the two mirror setup and travels back nearly along the original direction of incidence. Fig. 1(a) illustrates how the laser beam travels between the spherical mirrors for 18 passes through the cell. It was impractical to make a drawing for 40 or more passes of the laser beam. The numbered dots within the sphere representing the spherical mirror at the bottom left of Fig. 1(a) indicate the positions of consecutive reflections of the laser beam. The laser beam travels from the left to the right edge of the spherical mirror *SM*1 and changes direction after the fifth reflection. If there were 40 passes before leaving the cell, the beam would change direction on the 10th reflection. In the illustrated example of 18 passes, the laser beam leaves the multi-pass system after the 9th reflection from mirror *SM*1. Diaphragms *D*1 and *D*2 block the beam from coming back to the laser diode.

2.3. Spectrometer

The Raman scattered light was collected by multi element uncoated condenser *L*2 made of Borosilicate Crown Glass, with *f*/# 0.7 collection angle with back focal length about 25 mm. The clear aperture of the lens *L*2 was about 60 mm, and transmission at 780 nm, at normal incidence was approximately 65%. Light was focused on the entrance slit of the 0.275-m Turner–Czerny spectrograph by a 50-mm diameter and 200-mm focal length plano convex lens *L*3. The diameter of focusing lens *L*3 was chosen to obtain best image quality at the entrance slit of the spectrograph. The imaging optics matched closely the *f*/#4 number of the spectrograph. Overall magnification of the collection optics was about 8. The grating used in all measurements has 600 grooves/mm and is blazed at 1.0 μm. The resulting resolution was 0.2 nm. The spectrograph was mounted on its side with entrance slit parallel to the laser beam in the sample cell. This arrangement images approximately 20 μm × 0.8 mm of focused laser beams area in the sample cell onto the 160 μm × 6 mm entrance slit of the spectrograph. This eliminated the need to rotate an image in order to increase the light collection efficiency from the scattering volume.

Back illuminated Hamamatsu CCD array of 1024 × 256, 24 μm pixels with well capacity of 300,000 electrons per pixel, cooled to 243 K was used as a light detector. Dark electron count at 243 K was about 10 electrons per pixel per second. The mechanical shutter is mounted in front of the entrance slit of the spectrograph. Most spectra were taken with exposure time between 1.0 min and 5.0 min. At low concentration the spectra were processed by adding of individual CCD readouts for a total acquisition time of 15–20 min.

3. Results

For a test case we used the sample of hydrogen isotopes at thermal equilibrium analyzed in house by means of mass spectrometry with H_2:D_2:HD ratio 2.8:100:19.9. The pure rotational Stokes Raman spectrum of this sample obtained with our apparatus is shown in Fig. 2. The spectrum was taken at room temperature of about 295 K at pressure of 1.3×10^4 Pa (number density $3.2 \times 10^{24}\,m^{-3}$). The spectrum shown in Fig. 2, is corrected for response function of the spectrograph and CCD camera which was determined with a calibrated tungsten source. We found it rather difficult to measure accurately the spectrograph/CCD response function due to etaloning effect of the back thinned CCD chip. The measured intensity of the tungsten source as a function of the wavelength in the spectral range between 780 and 860 nm varied significantly with small position adjustments of the light source. The variation in sensitivity response curve were up to 8% per 5 nm depending on the position of the light source. The identification of spectral lines is after reference [10,11]. The numbers in parenthesis by each spectral line denote initial rotational quantum number. The D_2 lines originating from *even* and *odd* rotational quantum numbers *J* alternate in intensities due to nuclear spin factor ratio $gJ_{\mathrm{even}}/gJ_{\mathrm{odd}} = 2$. The unfiltered remnants of Rayleigh line at 780 nm were artificially removed from the spectrum in Fig. 2 and the background was subtracted to bring the baseline to zero counts.

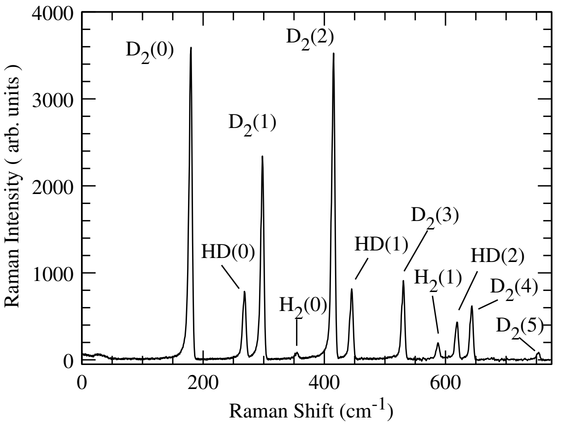

Fig. 2. Pure rotational Stokes Raman spectrum. The mixture of hydrogen isotopes H_2:D_2:HD with number density ratio 2.8:100:19.9 at room temperature and total pressure of about 1.3×10^4 Pa (number density $3.2 \times 10^{24} m^{-3}$). The numbers in parenthesis denote initial rotational quantum number.

The quantities monitored are the relative number densities of hydrogen isotopes as the ratio of each isotopic species to total number density of all gases combined. We will refer to that ratio as Γ throughout the paper. Note that the Raman cross sections are independent of the isotopic constituents of the hydrogenic molecules.

The relationship between number densities and Raman intensities are described in the Appendix A. We show there that if sufficient number of spectral lines are included in analysis then:

$$\Gamma_{\mathrm{HD}} = \frac{I(\mathrm{HD})}{I(\mathrm{D}_2) + I(\mathrm{H}_2) + I(\mathrm{HD})}, \tag{1}$$

where I(HD), $I(D_2)$,$I(H_2)$ are sums of integrated intensities (areas) under all spectral lines of the hydrogen isotopes. Therefore the quantity we report from here on, is not actual the ratios of number densities but the ratio of sums of integrated Raman intensities (areas) under all lines of each isotopic species. The method used for evaluating integrated intensities (areas) is described in the Appendix B.

For our test gas sample the value for Γ_{HD}, computed from integrated intensities under Raman lines as defined by equation (2) is equal to 0.168 ± 0.002 versus 0.163 obtained from the mass spectra measurements of unknown accuracy.

3.1. Sensitivity determination

The accurate quantitative determination of the amounts of species based on spectroscopic methods requires that no significant interference with neighboring spectral lines occurs. For the system studied here, most, but not all spectral features which belong to pure rotational S-band of all hydrogen isotopes are well isolated. The sensitivity of our spectrometer is demonstrated in

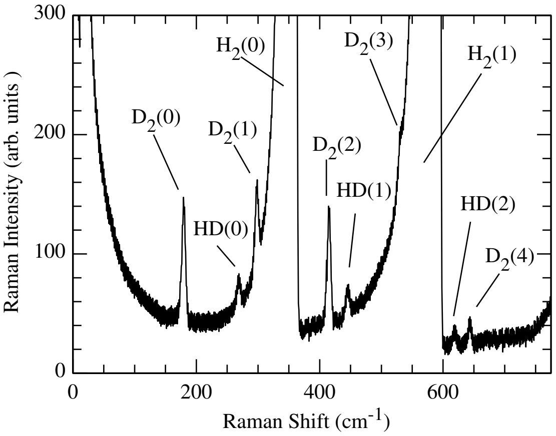

Fig. 3. The same Raman spectrum as shown in Fig. 2. The total gas pressure is equal to 5.3×10^4 Pa (number density $1.3 \times 10^{25} m^{-3}$). The number density ratio of H_2:D_2:HD is 4000:5:1.

Fig. 3. The spectrum in Fig. 3 is addition of 4, five minutes CCD exposures. The 370 mW laser beam traveled 46 times between mirrors *SM*1 and *SM*2. The gas sample was prepared by filling the evacuated cell by a mass analyzed mixture H_2:D_2:HD with ratio 2.8:100:19.9 to pressure equal to 80 Pa (number density $2.0 \times 10^{22} m^{-3}$). This resulted with 13.3 Pa (number density $3.3 \times 10^{21} m^{-3}$) pressure of HD and 66.6 Pa (number density $1.6 \times 10^{22} m^{-3}$) D_2 in the cell. The pressure was monitored by calibrated capacitance manometer accurate to 0.25%. Next, the cell was filled to total pressure of 5.3×10^4 Pa (number density $1.3 \times 10^{25} m^{-3}$) by adding pure H_2 gas. The estimated number density ratio of H_2:D_2:HD in the cell was 4000:5:1 Several Raman lines which belong to HD are easily identified with the signal-to-noise ratio better than 2. Well above a value of 1 usually defined as the detection limit.

We concluded that the overlapping rotational Raman lines from different isotopes are limiting factor in detection of trace amounts of HD. The accurate identification of hydrogen isotopes at concentrations much smaller than 1:4000 would require a spectrograph with higher resolution than the one we had available.

3.2. Isotope exchange

Formation of HD molecules as a result of interaction between the material surface and gaseous hydrogen isotopes mixtures of H_2, D_2 is governed by the isotopic exchange reaction:

$$H_2 + D_2 \rightleftharpoons 2HD \tag{2}$$

After enough time the system will come to thermal equilibrium. At equilibrium the number densities of the isotopes satisfy the relation below.

$$K(T) = \frac{n_{HD}^2}{n_{H_2} n_{D_2}} \tag{3}$$

where n_{HD},n_{H_2}, and n_{D_2} are number densities of HD, H_2 and D_2 after thermodynamic equilibrium has been reached. Equilibrium constant $K(T)$ can be calculated in terms of partition functions [12] and is equal to 3.28 at 300 K and 3.75 at 700 K which is equal to temperature of palladium membrane. Additionally if we assume that total number of hydrogen and deuterium atoms is unchanged in time, the set of equations below allow us to predict number densities of HD, H_2 and D_2 after thermodynamic equilibrium has been reached.

$$K(T) = \frac{n_{HD}^2}{n_{H_2} n_{D_2}} \tag{4}$$

$$n_{H_2} + \frac{1}{2} n_{HD} = \alpha \tag{5}$$

$$n_{D_2} + \frac{1}{2} n_{HD} = \beta, \tag{6}$$

where $2{*}\alpha$ and $2{*}\beta$ are initial numbers of hydrogen and deuterium atoms.

We performed a series of measurements to determine rates of isotope exchange reactions in our gas handling system under two conditions:

1. When the hydrogen purifier was not a part of gas recycling system.
2. When the palladium membrane hydrogen purifier was a part of the flow system.

First the system was filled with a mixture of H_2, D_2 and HD gases through valve *V*3 to a total pressure of 4.0×10^4 Pa (number density $9.8 \times 10^{24} m^{-3}$) with number densities ratio 100:100:20. The temperature was 295 K. We closed all the valves and measure pure rotational Raman spectrum similar to one shown in Fig. 2.

The partial pressure ratio Γ_{HD} of hydrogen isotopes inferred from the sum of integrated spectral lines was evaluated. The spectral measurements at equal time intervals were repeated over 12 days. The $\Gamma_{HD} \times 100$ is plotted as a function of time in Fig. 4. Each point in Fig. 4 is an average of 3 experiments. The total intensity of the entire spectrum changed from day to day but ratio Γ_{HD} remains the same. The concentration of Γ_{HD} inferred from Raman spectra was approximately equal to 9.4% versus 9.1% concentration estimated from reading of partial pressures. The equilibrium value for Γ_{HD} computed from Eqs. (4)–(6) at 295 K is 0.46 for gas composition used in our experiment.

Within the accuracy of our measurements (around than 1%) we detected no additional formation of HD. The largest contribution to the error in Γ_{HD} are due to uncertainty in determination of the background level in the Raman spectra. We describe in detail methods

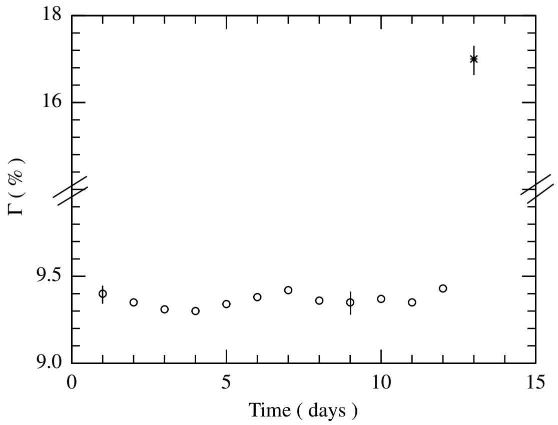

Fig. 4. Concentration of HD molecules in HD/D_2/H_2 mixture as a function of time. The rapid change at the end of the graph took place after introducing palladium purifier into the system. The vertical lines illustrate typical estimated error.

use for data analysis in Appendix B. The surfaces in the gas handling system are made out of stainless steel and glass. The gaskets are made from copper. The sytem was heated overnight at 530 K before experiments.

Next we passed the identical composition of gasses through the palladium purifier through valve *V*2 and *V*1 while keeping valve *V*3 closed, and take spectral measurements. The coefficient Γ_{HD} increases instantly following passage of the gas through palladium membrane. We note that one has to operate palladium purifier for several minutes at 630 K before steady value of Γ_{HD} is established. The HD concentration increased by less than 10% just after the purifier was turned on. The steady state value of Γ_{HD} reached 17% after the passage of the gas through hot palladium membrane. This change indicates increase in HD number density by almost factor of 2. The HD concentration at thermodynamical equilibrium at 700 K is equal to 50%. After one passage through Pd membrane concentration of HD reaches 34% of equilibrium value. Our expectation was that the gas will reach thermodynamical equilibrium. Recent measurements of co-permeation of deuterium and hydrogen through palladium at low pressure [3] performed under carefully controlled environment indicate that mixture of hydrogen and deuterium comes to thermal equilibrium following one passage through the hot Pd membrane. However, authors in reference [3] note deviation from equilibrium with rising pressure. This makes it difficult to compare our results with ones by Kizu [3] since we operated at pressures up to 100 times higher.

4. Conclusions

We have designed and built simple, relatively inexpensive Raman spectrometer for monitoring isotope exchange in hydrogen gas. With this spectrometer we have demonstrated: (1) Partial pressures of hydrogen isotopes at total gas pressures of 5.3×10^4 Pa (number density $1.3 \times 10^{25}\mathrm{m}^{-3}$) could be monitored at levels 13 Pa (number density $3.2 \times 10^{21}\mathrm{m}^{-3}$) during minutes long observations. (2) Formation of HD in D_2, H_2 mixtures can be monitored with accuracy about 1%.

Acknowledgement

Support from NSF is gratefully acknowledged. At MTU financial assistance from Dean of College of Sciences and Arts and VP for research is much appreciated. The authors thank Bob Michie for a critical review of the manuscript.

Appendix A

The intensity *I* for pure rotational Raman spectra of a diatomic molecule for *S* band ($\Delta J = +2$) is proportional to: [13]

$$I \alpha g_N v_s^4 N_i b_{J+2,J}^{(2)}, \tag{7}$$

where *J* is the initial rotational quantum number, v_s is a frequency of Raman line, g_N is a nuclear spin degeneracy factor, $b_{J+2,J}^{(2)}$ is a Placzek–Teller factor equal to:

$$b_{J+2,J}^{(2)} = \frac{3(J+1)(J+2)}{3(2J+1)(2J+3)}, \tag{8}$$

and N_i is a population factor given by:

$$N_i = \frac{N(2J+1)\exp(-BJ(J+1)/kT)}{\Sigma(2J+1)\exp(-BJ(J+1)/kT)}. \tag{9}$$

N is a total number of molecules of given kind, *B* is rotational constant, *k* is a Boltzman constant, and *T* is temperature, *kT* at 300 K is equal to 208 cm^{-1}. The nuclear spin degeneracy factor g_N is equal to:

(1) for H_2, 3 for *J* odd and 1 for *J* even;
(2) for D_2, 1 for *J* odd and 2 for *J* even;
(3) for HD is equal 1 for both odd and even values of *J*.

Appendix B

The Raman line shape measured with instrument of unlimited resolution is a combination of Doppler and pressure broadening and is well represented by Voigt profile. The expected width of resulting Voigt profile at our range of pressures and room temperature is about 5 GHz which is very small in comparison to our instrumental resolution of 90 GHz.

The optimal method to evaluate integrated intensity under each Raman peak is to use nonlinear fitting routine to fit each line to the spectrometer response function. This approach allows also for straightforward quantification of errors.

Unfortunately, our spectrometer images the entrance slit onto the complex asymmetric curve producing spectral lines which are difficult to represent by simple analytical function. Therefore we opted for less accurate but very quick manual method of evaluating integrated intensities (areas under spectral lines). We are aware that this method is suitable for well isolated peaks only, like from hydrogen isotopes. We manually define the left and right edges of each peak and integrate the base line corrected area under the peak. The result is the sum of the intensities between selected left and right edges. We call it integrated Raman intensity throughout the paper. We found that the choice of the method of baseline correction (leveling) was a limiting factor in error reduction of measuring the partial pressure of any hydrogen isotopes. Two methods of leveling the spectra was used:

1. Multiple point baseline correction. In this method we fitted line segments between multiple points on X axis. The points were chosen manually and didn't belong to any of the spectral peaks. Up to 15 points were used.
2. Polynomial cure fit baseline correction. In this method we fitted polynomials up to order 5 to the data points manually chosen which by our judgment didn't belong to any of the spectral peaks.

Depending on the method and points selected to be used in baseline correction procedure we arrived with different ratios of integrated Raman intensities. The error bars shown in Fig. 4 are actual spread of results obtained from three different experiments using at least 2 different choices of baseline correction procedures. Therefore the error bars reperesent the maximum error.

References

[1] D. Ducret, C. Laquerbe, A. Ballanger, J. Steimetz, V. Porri, J.P. Verdin, T. Pelletier, Fusion Sci. Technol. 41 (2002) 1092.
[2] A.A. Pisarev, P.O. Kokurin, Yu.V. Borisyuk, Tech. Phys. Lett. 24 (1998) 924.
[3] Kaname Kizu, Alexander Pisarev, Tetsuo Tanabe, J. Nucl. Mater. 289 (2001) 291.
[4] A. Zuttel, Ch. Nutzenadel, G. Schmid, Ch. Emmenegger, P. Sudan, L. Schlapbach, Appl. Surf. Sci. 162–163 (2000) 571.
[5] David J. Taylor, Manfred Glugla, Ralf-Dieter Penzhorn, Rev. Sci. Instr. 72 (2001) 1970.
[6] J.C. Robinson, M. Fink, A. Mihill, Rev. Sci. Instrum. 63 (1992) 3280.
[7] J. Sabbaghzadeh, W. Buell, J. Holder, M. Fink, Appl. Phys. B 60 (1995) 261.
[8] W. Kiefer, H.J. Bernstein, H. Wieser, M. Danyluk, J. Mol. Spectrosc. 43 (1972) 393.
[9] R. Claps, J. Sabbaghzadeh, M. Fink, Appl. Spectroscopy 53 (1999) 491.
[10] H. Herzberg, Molecular Spectra and Molecular Structure, Van Nostrand, New York, 1950.
[11] D. Kirk Veirs, Gerd M. Rosenblatt, J. Mol. Spectrosc. 121 (1987) 401.
[12] Donald A. McQuarrie, Statistical Mechanics, Harper Collins Publishers, 1972.
[13] Derek E. Long, Raman Effect: A Unified Treatment of the Theory of Raman Scattering by Molecules, John Wiley & Sons Ltd., 2002.